THE JOURNAL OF BIOLOGICAL CHEMISTRY VOL. 281, NO. 37, pp. 27278–27285, September 15, 2006

Screening-based Discovery and Structural Dissection of a Novel Family 18 Chitinase Inhibitor*

Received for publication, April 24, 2006, and in revised form, June 19, 2006 Published, JBC Papers in Press, July 14, 2006, DOI 10.1074/jbc.M604048200

Alexander W. Schüttelkopf[‡], Ole A. Andersen[‡], Francesco V. Rao[‡1], Matthew Allwood[‡2], Clare Lloyd[§], Ian M. Eggleston[‡], and Daan M. F. van Aalten[‡3]

From the [‡]Division of Biological Chemistry and Molecular Microbiology, Wellcome Trust Biocentre, School of Life Sciences, University of Dundee, Dow Street, Dundee DD1 5EH, Scotland and the [§]Leukocyte Biology Section, Faculty of Medicine, Imperial College London, London SW7 2AZ, United Kingdom

Family 18 chitinases play key roles in the life cycles of a variety of organisms ranging from bacteria to man. Very recently it has been shown that one of the mammalian chitinases is highly overexpressed in the asthmatic lung and contributes to the pathogenic process through recruitment of inflammatory cells. Although several potent natural product chitinase inhibitors have been identified, their chemotherapeutic potential or their use as cell biological tools is limited due to their size, complex chemistry, and limited availability. We describe a virtual screening-based approach to identification of a novel, purine-based, chitinase inhibitor. This inhibitor acts in the low micromolar ($K_i = 2.8 \pm 0.2$ μM) range in a competitive mode. Dissection of the binding mode by x-ray crystallography reveals that the compound, which consists of two linked caffeine moieties, binds in the active site through extensive and not previously observed stacking interactions with conserved, solvent exposed tryptophans. Such exposed aromatics are also present in the structures of many other carbohydrate processing enzymes. The compound exhibits favorable chemical properties and is likely to be useful as a general scaffold for development of pan-family 18 chitinase inhibitors.

Family 18 chitinases (CAZy GH 18) hydrolyze chitin, a homopolymer of β-(1,4)-linked *N*-acetylglucosamine. Chitin is a key component of the fungal cell wall, and chitinases are thought to be required for fungal cell separation and morphogenesis (2–4). Strikingly, whereas chitin does not occur in humans, it is known that we possess two chitinases (5, 6). Human macrophage chitotriosidase (HCHT)[4] is secreted by activated macrophages and is able to degrade chitin from the cell wall of the fungal pathogen *Candida albicans*. Although its precise role has not been defined, it has been shown to be upregulated during fungal or bacterial infection (7) and Gaucher disease, a lysosomal storage disorder (8). A second chitinase, termed acidic mammalian chitinase was subsequently discovered and shown to possess an unusually low pH optimum (<3) (6), and its overexpression in the lung has been linked to the progression of asthma.

Most known family 18 chitinase inhibitors are natural products (reviewed in Ref. 9), including the cyclic dipeptide CI-4 and related compounds (10, 11), the cyclic pentapeptides argifin and argadin (12–14), and the pseudotrisaccharide allosamidin, a nanomolar inhibitor isolated from *Streptomyces* sp. (15). Their poor synthetic accessibility and limited availability from natural sources has so far hampered the use of these inhibitors for *in vivo* studies, whereas their chemical complexity makes them unsuitable as starting points for ligand design efforts. Nevertheless, numerous crystallographic and biochemical studies have elucidated the interactions between these compounds and family 18 chitinases (*e.g.* Refs. 11, 14, and 16–18).

Recently, a high throughput screen identified three xanthine derivatives, theophylline, caffeine, and pentoxifylline, as competitive inhibitors of bacterial, fungal, and human family 18 chitinases (19). Although their inhibition was not strong (high micromolar), analysis of their mode of inhibition revealed that these molecules mimic many of the chitinase-substrate hydrogen bonds and in addition display extensive π-π stacking interactions with a conserved tryptophan. Here, we describe a simple, fragment-based approach to virtual screening of commercially available chemical structures, starting from the caffeine scaffold. The virtual screen resulted in the identification of a new xanthine-based chitinase ligand that competitively inhibits several family 18 chitinases in the low micromolar range.

EXPERIMENTAL PROCEDURES

LIGTOR: a Simple and Efficient Virtual Screening Algorithm—Several examples of successful fragment-based drug discovery have recently been reported (reviewed in Refs. 20 and 21). The approach is to identify binding modes of very small, but highly efficient, chemical entities, which are then further elaborated or connected together through small linkers to yield dramatic increases in inhibition. Unfortunately, no freely available, noncommercial programs for such elaboration of fragments have

* The costs of publication of this article were defrayed in part by the payment of page charges. This article must therefore be hereby marked "*advertisement*" in accordance with 18 U.S.C. Section 1734 solely to indicate this fact.

The atomic coordinates and structure factors (code 2IUZ) have been deposited in the Protein Data Bank, Research Collaboratory for Structural Bioinformatics, Rutgers University, New Brunswick, NJ (http://www.rcsb.org/).

[1] Supported by a British Biomedical Research Support Group CASE studentship together with Syngenta.

[2] Supported by a Wellcome Trust studentship.

[3] Supported by a Wellcome Trust Senior Research Fellowship and the European Union FP6 FUNGWALL STREP. To whom correspondence should be addressed. Tel.: 44-1382-344979; Fax: 44-1382-345764; E-mail: dava@davapc1.bioch.dundee.ac.uk.

[4] The abbreviations used are: HCHT, human macrophage chitotriosidase; 4MU-GlcNAc$_2$, 4-methylumbelliferyl-β-D-*N*,*N*′-diacetylchitobiose; 4MU-GlcNAc$_3$, 4-methylumbelliferyl-β-D-*N*,*N*′,*N*″-triacetylchitobiose; r.m.s., root mean square; *Af*ChiB1, *Aspergillus fumigatus* chitinase B1; *Sm*ChiA, *Serratia marcescens* chitinase A.

so far been reported. Here we describe LIGTOR, a program for rapidly evaluating compounds starting from a two-dimensional library of chemical molecules and a structurally characterized starting fragment. As a first step, a virtual compound library was searched for molecules containing the fragment as a substructure; depending on the choice of fragment, this step will leave only a small number of compounds for consideration. Using the fragment structure as a template, chemically sensible three-dimensional coordinates are generated for the selected compounds, so that orientation and conformation of the fragment-equivalent substructure matches that of the template as closely as possible, even if the molecules differ in atom or bond types due to degeneracy in the search pattern. If a library compound contains more than one instance of the fragment substructure, several coordinate sets are produced. These initial binding modes are then optimized by evaluation of torsion angles (outside the fragment substructure) and, optionally, the overall position/orientation in the context of the protein receptor. Subsequently, compounds with poor predicted binding or excessive coordinate shifts of their fragment substructure are discarded. The docked complexes of the remaining compounds are inspected visually, promising candidates are chosen for *in vitro* testing and cocrystallization.

The substructure search is carried out with SDFSCAN, a command-line tool for selecting compounds from a library by (sub-)structure; SDFSCAN accepts input either in SDFile format or in an enriched SDFSCAN-specific format that can be generated using PRODRG (22). Template-based coordinate generation is also performed with PRODRG. Ligands are docked using LIGTOR, a PRODRG extension for evaluating and optimizing ligand poses against a receptor described by affinity grid maps. Currently, LIGTOR uses the AutoDock 3.0 force field (23) with a modified ligand-internal energy term to accelerate computation. Another difference to AutoDock is that LIGTOR minimizes the predicted ΔG, not ΔH. LIGTOR obtains ligand descriptions including a list of optimizable torsion angles from PRODRG. Depending on the application, LIGTOR can also optimize the overall position/orientation of the ligand or, alternatively, keep a part of the ligand (in this case the fragment substructure) fixed. In the former case harmonic restraints may be applied to either the coordinates of a substructure or to the center of mass of parts/all of the ligand. Instructions for obtaining SDFSCAN, LIGTOR, and PRODRG are available upon request.

Protein Purification and Enzyme Assays—Chitinase B1 from *Aspergillus fumigatus* (*Af*ChiB1) was overexpressed in *Escherichia coli* and purified as described previously (19). Selected hits from the virtual screen against *Af*ChiB1 were purchased from suppliers indicated in Table 1. C_2-dicaffeine was later re-synthesized according to the method of Cavallaro *et al.* (24). The compound was characterized by ^{1}H and ^{13}C NMR and electrospray mass spectrometry, and its purity confirmed by analytical reverse phase-high performance liquid chromatography.

Enzyme activity was determined using 4-methylumbelliferyl-β-D-*N*,*N*′-diacetylchitobiose (4MU-$GlcNAc_2$; Sigma) or 4-methylumbelliferyl-β-D-*N*,*N*′,*N*″-triacetylchitobiose (4MU-$GlcNAc_3$; Sigma) as substrates in a standard assay as described previously (5, 18, 19). In a final volume of 50 μl, 5 nM enzyme was incubated with 20 μM substrate in McIlvain buffer (100 mM citric acid, 250 mM sodium phosphate, pH 5.5) containing 0.25 mg/ml bovine serum albumin for 10 min at 37 °C in the presence of different concentrations of inhibitor. 5–30 μM 4MU-$GlcNAc_2$ was used for determination of K_i for C_2-dicaffeine against *Af*ChiB1. Experiments were performed in triplicate. Production of 4MU was linear for the incubation period used, and less than 10% of available substrate was hydrolyzed. Kinetic data were fitted with GRAFIT 5.0 (25) against standard equations for dose-response curves and competitive inhibition. A similar approach was employed to evaluate inhibition against the human chitotriosidase (22 μM 4MU-$GlcNAc_3$, 0.4 nM enzyme) and chitinase A from *Serratia marcescens* (60 μM 4MU-$GlcNAc_2$, ≈7.4 nM enzyme; Sigma).

Crystallization and Structure Determination—Crystals of *Af*ChiB1 were grown by vapor diffusion from 0.1 M Tris/HCl, pH 9.5, and 1.4 M Li_2SO_4. Crystals were washed three times in 0.1 M sodium citrate, pH 5.5, and 1.4 M Li_2SO_4, then soaked for 25 min in mother liquor containing ≈125-fold molar excess of C_2-dicaffeine before cryoprotection in 3 M Li_2SO_4. Data were collected at beamline BM14, European Synchrotron Radiation Facility (ESRF), and processed with the HKL suite (26). Refinement was started from the native *Af*ChiB1 structure (Protein Data Bank code 1W9P) and proceeded through cycles of model building with O (27) and positional/*B*-factor refinement using REFMAC (28). A model for C_2-dicaffeine was not included until completely defined by the unbiased $|F_o| - |F_c|$, φ_{calc} electron-density maps (Fig. 1*C*). Ligand starting structure and topology were generated with PRODRG (22). Data and refinement statistics are given in Table 2. Fig. 1 was rendered with PyMOL.

RESULTS

Identification of Elaborated 3-Methylxanthines by Virtual Screening—Recently, three 1,3-dimethylxanthine derivatives, theophylline, caffeine, and pentoxifylline (Fig. 1*A*), were identified as inhibitors of *A. fumigatus* chitinase B1 (*Af*ChiB1) in a high throughput screen (19). Despite their relatively poor affinity (K_i = 37 μM for pentoxifylline), these compounds present interesting starting points for ligand design, as they displayed a common binding mode, not previously observed in family 18 chitinase inhibitors, involving extensive π-π stacking interactions with a fully conserved tryptophan and mimicry of chitinase-substrate hydrogen bonds (Fig. 1). Furthermore, these compounds show good ligand efficiency (expressed as ΔG per non-hydrogen atom (29), $\Delta g = -0.43$ kcal mol^{-1} atom^{-1} for pentoxifylline) and are easy to synthesize or derivatize. The rigid xanthine moiety of the three compounds binds in a virtually identical orientation to the *Af*ChiB1 active site (19), making it an ideal starting point for further optimization.

From a chemical point of view, further functionalization of the xanthine scaffold is mainly possible at four positions: at N-1, N-3, N-7, and C-8 (Fig. 2*A*). However, the binding mode of the xanthine suggests that of these, modification at N-7 and C-8 is restricted as these both point toward small cavities in the structure. In comparison, both N-1 and, to a lesser extent N-3, should be able to accept larger modifications (Fig. 1*A*). The

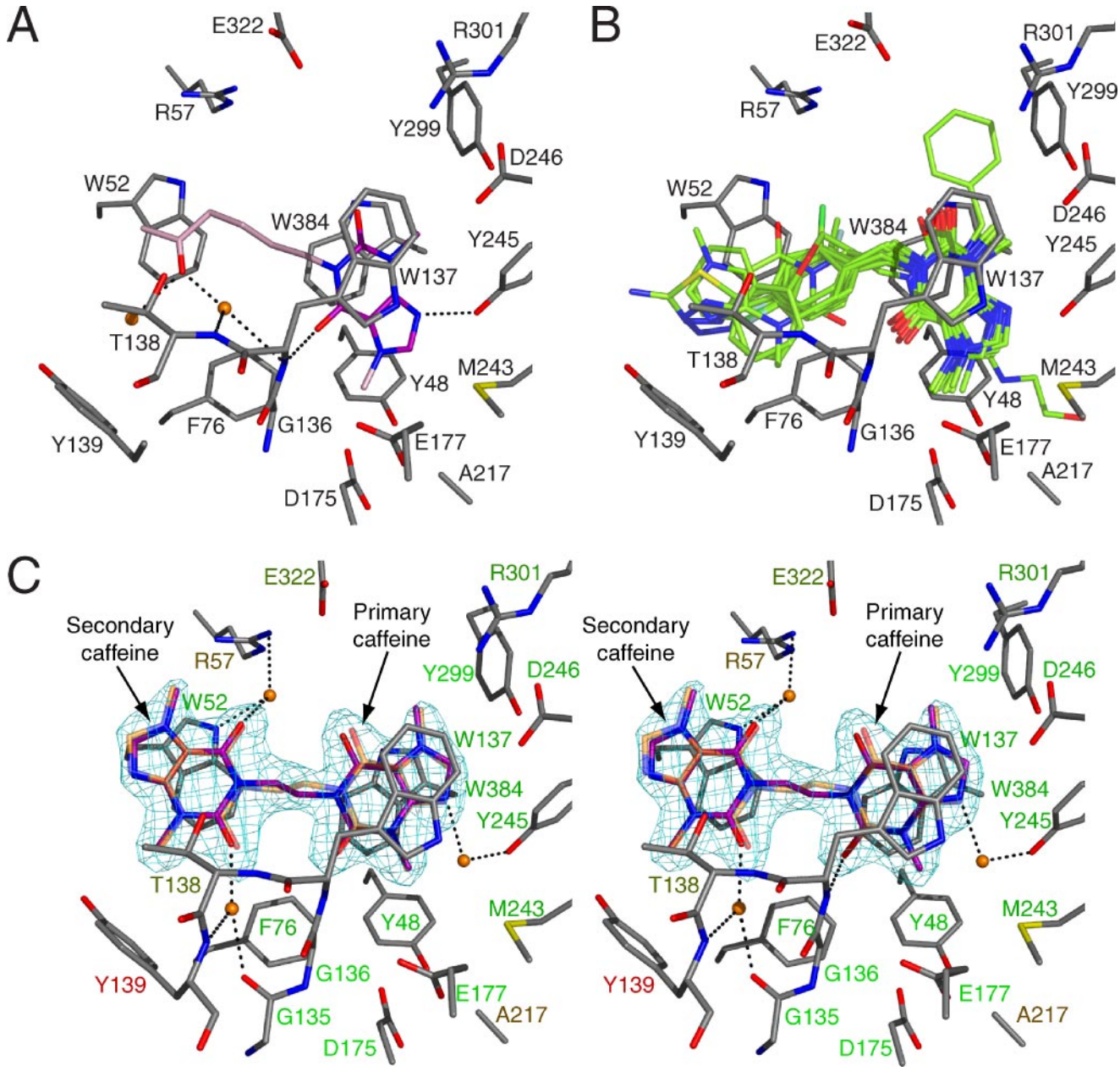

FIGURE 1. **The active site of *Af*ChiB1 in complex with xanthine derivatives.** Active site residues are shown as *gray stick models*, possible hydrogen bonds are indicated by *dotted black lines*, crystallographic waters interacting with ligands are shown as *orange spheres*. *A*, the crystallographic complex with pentoxifylline (*purple*) (19), which provided the starting point for virtual screening. The 3-methylxanthine moiety used as the rigid fragment is shown *dark*, whereas the 7-methyl group and the oxohexyl tail are *lighter*. *B*, the docked conformations (*pale green*) of the compounds are listed in Table 2. Possible hydrogen bonds have been omitted. *C*, crystal structure of the *Af*ChiB1-C_2-dicaffeine complex (stereo). The major conformation of the ligand is shown in *purple*, the minor ($q = 0.25$) conformation is shown semitransparently in *orange*. The unbiased $|F_o| - |F_c|$, φ_c electron density map is shown contoured at 2.5 σ. The label color indicates conservation of the corresponding residue among bacterial-like family 18 chitinases using a color gradient from *red* (not conserved) to *green* (completely conserved): to evaluate sequence conservation, a list of family 18 glycoside hydrolases was obtained from CAZy. After removing entries not marked as chitinases (EC 3.2.1.14) and entries lacking a full-length UniProt entry, sequences were downloaded from UniProt and aligned with ClustalW (1). Elimination of sequences lacking the active site motif D*XX*D*X*D*X*E yielded 165 putative chitinase sequences, which were separated by sequence length into 129 bacterial-like chitinases (proteins longer than 370 amino acids) and 36 plant-like chitinases (proteins shorter than 370 amino acids).

oxohexyl group of pentoxifylline is an example for such a modification on N-1 (Fig. 1*A*) and its presence improves binding to *Af*ChiB1 almost 4-fold (19).

Purine scaffolds have been extensively used in inhibitor design (*e.g.* Refs. 30–33). We searched a data base of 5.1 million commercially available compounds for molecules containing a 3-methylxanthine substructure, identifying 50,193 candidate ligands. We then evaluated all these ligands using the LIGTOR program developed as part of this study (see "Experimental Procedures"). The coordinates of the 3-methylxanthine substructure were kept fixed while performing a torsional evaluation of the substitutions, in the context of the protein component of the published *Af*ChiB1-pentoxifylline complex (19) as the receptor. After docking with PRODRG/LIGTOR, compounds were selected by predicted free enthalpy of binding ($\Delta G < -10.0$ kcal mol^{-1}),

TABLE 1

Compounds selected for testing against *Af*ChiB$_1$, sorted by predicted affinity

Compound numbers refer to Fig. 2*A*. The IC_{50} for pentoxifylline is taken from Ref. 19. Rank and r.m.s. deviations (in Å) pertain to the *ab initio* docking and are explained in the text.

Compound	Supplier	ΔG_{pred} [a]	Δg_{pred} [b]	$IC_{50,exp}$ [c]	Rank	r.m.s. deviation
2	Chembridge	−13.42	−0.48	4.8 ± 1.4	1	0.256
3	Specs	−13.07	−0.45	NA[d]	7	2.051
4	Chembridge	−12.84	−0.46	>1000	2	1.056
5	Specs	−12.73	−0.58	520 ± 80	1	1.050
6	Specs	−12.72	−0.49	>1000	2	0.515
7	Specs	−11.73	−0.43	>1000	1	0.591
1, $R_1 = -F$, $R_2 = -Cl$	Chembridge	−11.45	−0.52	>1000	1	0.371
8	Sigma	−10.91	−0.55	126 ± 7	1	0.211
9	IBS	−10.86	−0.52	NA	1	0.843
1, $R_1 = -H$, $R_2 = -CH_3$	Chembridge	−10.84	−0.52	>1000	1	0.174
1, $R_1 = -H$, $R_2 = -F$	Chembridge	−10.77	−0.51	>1000	1	0.142
1, $R_1 = R_2 = -H$	Chembridge	−10.68	−0.53	>1000	1	0.176
10	Specs	−10.48	−0.52	NA	2	0.279

[a] ΔG_{pred} = predicted free enthalpy of binding in kcal mol^{-1}.
[b] Δg_{pred} = ligand efficiency in kcal mol^{-1} atom^{-1}.
[c] $IC_{50,exp}$ = experimental IC_{50} in μM.
[d] NA, not available.

predicted ligand efficiency ($\Delta g < -0.35$ kcal mol^{-1} atom^{-1}), and coordinate shift of the 3-methylxanthine substructure atoms (r.m.s. deviation between starting and docked conformations <0.6 Å). The predicted conformations of the 263 unique compounds fulfilling all three criteria were inspected visually and finally the 12 compounds listed in Table 1 were purchased for *in vitro* testing. The docked conformations for these compounds are shown together in Fig. 1*B*.

Desirable Chemical Features Are Enriched in the Virtual Screening Hits—A question in assessing the validity of the virtual screening approach is to what extent the docking-based compound selection leads to an enrichment of the discussed features (small groups on N-7/C-8, larger groups on N-1/N-3), especially as the set of 50,193 xanthine derivatives that serve as the starting point show an unfavorable distribution of functionalizations: less than 9% of the compounds carry more than one non-hydrogen atom on N-1, whereas 90% and 88% of all compounds have undesirably large groups attached to N-7 and C-8, respectively (Fig. 2*B*). However, analysis of the group size distributions for the set of 263 compounds selected after docking shows, as expected, a clear preference for large modifications on N-1 (97% of the set carry two or more attached non-hydrogen atoms) and at slight preference for large modifications on N-3 (Fig. 2*B*). Similarly, the expected restrictions were on substitutions on N-7 (over 95% of the selected compounds are modified with a single non-hydrogen atom) and C-8 (a relative increase of unmodified compounds, although more than half of the selected molecules still carry a "heavy" modification). In conclusion, the set of functionalizations selected by the virtual screen are generally in agreement with the distribution expected based on experimental data and visual inspection of the active site.

The Virtual Screen Identifies a Low Micromolar Inhibitor—Twelve compounds from the selected set were chosen for *in vitro* evaluation (Fig. 2). They were picked to approximately represent the chemical features found in the entire set. Most of them have functional groups attached at N-1 that may interact with Trp^{52}, as observed in the pentoxifylline complex (Fig. 1*A*). One compound has a free N-7, the others present a methyl group at N-7. One compound each carries a large group on N-3 and C-8, otherwise these atoms are methylated or unmodified, respectively. The compounds are listed, with their predicted free enthalpy of binding and efficiency, in Table 1, as is pentoxifylline, which was also identified as a candidate ligand by the virtual screen.

Of the 12 compounds, three were not delivered by the suppliers, for the remaining compounds IC_{50} values for the inhibition of *Af*ChiB1 were determined. Only two of them, compounds **2** and **5** (Fig. 2*A*), showed significant inhibition. Compound **5** performs significantly worse than its parent compound caffeine and was not considered any further. Only compound **2** (1-(2-(theobromine-1-yl)ethyl)-theobromine, from here on referred to as C_2-dicaffeine) showed a significantly increased affinity to *Af*ChiB1. With an IC_{50} of 4.8 ± 1.4 μM it improves inhibition by 2 orders of magnitude compared with its parent compound (caffeine) and even when compared with pentoxifylline, so far the highest affinity purine-based chitinase inhibitor, it improves inhibition ≈25-fold.

C_2-dicaffeine Is a Competitive Inhibitor with an Extensive π-π Stacking Binding Mode—The inhibition of *Af*ChiB1 by C_2-dicaffeine was further investigated using kinetic measurements. Lineweaver-Burk analysis of steady-state kinetic experiments with varying substrate and inhibitor concentrations showed that C_2-dicaffeine is a competitive inhibitor of the chitinase with a K_i of 2.8 ± 0.2 μM (Fig. 2*C*). This makes it more than 1 order of magnitude more potent than pentoxifylline (K_i = 37 ± 2 μM (19)).

We next investigated the binding mode of C_2-dicaffeine by solving a high resolution crystal structure of the *Af*ChiB1-C_2-dicaffeine complex (Table 2, Fig. 1*C*). The active site Asp^{175} is pointing down into the catalytic core similarly to the other xanthine derivative complexes (r.m.s. deviation = 0.244 Å for 185 atoms of 19 active site residues comparing to the pentoxifylline complex). Defined electron density for C_2-dicaffeine shows the ligand bound to the protein in an overall orientation similar to that predicted by docking: the "primary" caffeine moiety is sandwiched between Trp^{137} and Trp^{384}, whereas the "secondary" caffeine stacks with Trp^{52} (Fig. 1*C*). The crystal structure also reveals two major differences from the known xanthine binding mode and the docked conformation: first, C_2-dicaf-

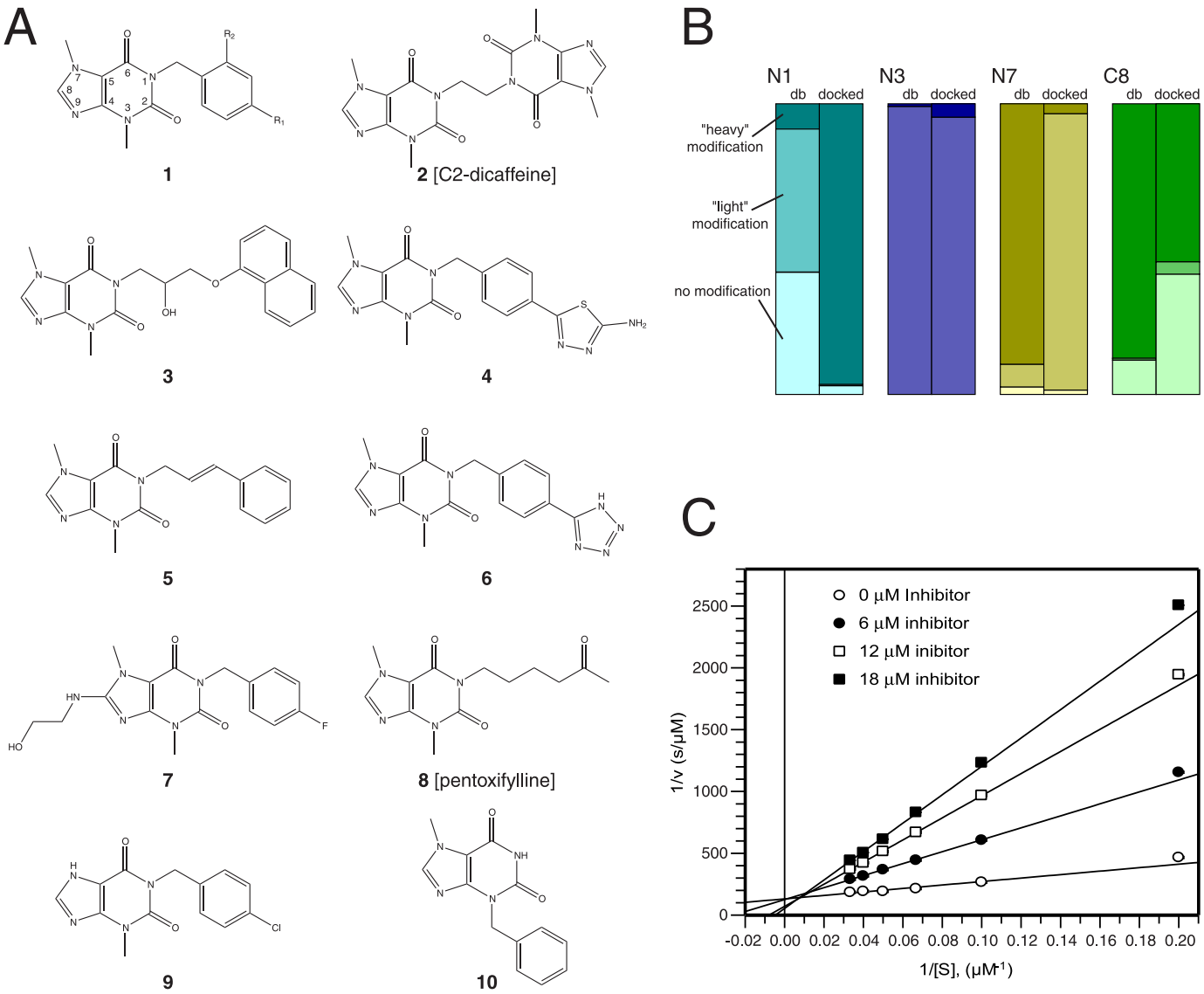

FIGURE 2. *A*, the chemical structures of the compounds discussed. Standard purine/xanthine atom numbering is shown for compound 1. *B*, enrichment of particular fragment structure modifications after docking. The *bars* show the size distributions for groups attached to N-1, N-3, N-7, and C-8 of the xanthine fragment structure for the set of 50,193 fragment search matches (labeled *db*) and the set of 263 docked compounds selected as possible ligands (labeled *docked*), distinguishing no attachment (*light color*; not for N-3), a single non-hydrogen atom (*medium color*), and more than one non-hydrogen atoms (*dark color*). *C*, Lineweaver-Burk plot of C_2-dicaffeine inhibition of *Af*ChiB1 at different concentrations. The data are compatible with a competitive inhibition model, giving a K_i of 2.8 ± 0.2 μM.

feine is shifted out of the active site by about 1.5 Å and second, both purine rings are flipped by 180° around their N-1 linker bond. This binding mode significantly improves π-π-stacking between the secondary caffeine and Trp^{52} compared with the docked orientation.

Similar to the other xanthine inhibitors the primary caffeine moiety of C_2-dicaffeine accepts two hydrogen bonds, one from the backbone amide of Trp^{137} and one from the hydroxyl of Tyr^{245}. Due to the flip of the ring system the former H-bond is formed by O-2 instead of O-6, and the direct interaction between Tyr^{245} and N-9 is replaced with a water-mediated hydrogen bond involving the same groups (Fig. 1*C*). O-2 of the secondary caffeine occupies a position similar to that of the pentoxifylline side chain carbonyl oxygen and, like it, accepts a hydrogen bond from a water molecule that in turn is held in place through interactions with the 136–139 loop forming one wall of the active site (Fig. 1, *A* and *C*). The secondary O-6 also hydrogen bonds to a water that interacts with the indole NH of Trp^{52} and the guanidino group of Arg^{57}.

Further inspection of the ligand electron density revealed it to be most compatible with the C_2-dicaffeine binding in a dual conformation. Refinement supported a major conformation with occupancy 0.75 and a minor conformation with occupancy 0.25. The two conformations are approximate mirror images of each other with the mirror plane being the average plane through all ligand atoms. This means that the two conformations occupy essentially the same space and form the same hydrogen bonds with the active site; the main differences between them are the tilt of the purine rings relative to their stacking partners and the torsion angles of the ethylene linker. The linker adopts a staggered conforma-

TABLE 2
Data collection and structure refinement statistics for the *Af*ChiB1-C_2-dicaffeine complex
Values in parentheses pertain to the highest resolution shell.

Data set	
Resolutions (Å)	20–1.95 (2.02–1.95)
No. of observed reflections	283,642 (25,771)
No. of unique reflections	96,150 (9,510)
Redundancy	2.9 (2.7)
$I/\sigma I$	21.0 (3.4)
Completeness (%)	99.2 (99.2)
R_{merge}	0.061 (0.452)
R_{work}, R_{free}	0.187, 0.223
r.m.s. deviation from ideal geometry	
Bonds (Å)	0.010
Angles (°)	1.5
B-factor r.m.s. deviation	
Bonds (main chain, Å^2)	1.6
Angles (main chain, Å^2)	2.1
$\langle B_{protein} \rangle$ (Å^2)[a]	24.2 ± 7.5
$\langle B_{ligand} \rangle$ (Å^2)	29.2 ± 2.6
$\langle B_{solvent} \rangle$ (Å^2)	35.6 ± 10.2

[a] Angle brackets are used to indicate that the values are averages.

tion, *i.e.* the central torsion angle is ~180°, whereas the torsion angles with the purine rings are ≈90° and −90° on either side. This linker conformation prevents the two caffeine rings from both achieving ideal stacking, the major ligand conformation has the primary caffeine significantly tilted against its tryptophan stacking partners (angle ≈19°), whereas the minor conformer has an unfavorable angle of over 23° between the Trp^{52} indole and its secondary caffeine. Together, the ligand shift/flip, the disorder and tilting of the aromatic systems, suggest that C_2-dicaffeine is in a strained conformation in the observed complex, which is non-ideal for tight binding.

C_2-dicaffeine Inhibits Several Family 18 Chitinases—Comparing the sequence of *Af*ChiB1 with that of other "bacterial-like" family 18 chitinases shows a high degree of conservation of the active site residues (Fig. 1*C*). With the exception of Thr^{138} and Tyr^{139}, all residues directly interacting with the C_2-dicaffeine ligand in the complex structure are conserved in >70% of known bacterial-like chitinases. In particular, the three tryptophan residues stacking with the aromatic systems of the ligand, Trp^{52}, Trp^{137}, and Trp^{384}, are conserved in >80% of sequences, suggesting that C_2-dicaffeine may be useful as a ligand for other bacterial-like family 18 chitinases. To investigate this possibility, three additional family 18 chitinases were assayed for inhibition by C_2-dicaffeine: HCHT, the acidic mammalian chitinase activity from mouse lung samples (*m*AMCase) and the bacterial chitinase A from *S. marcescens* (*Sm*ChiA).

The HCHT active site contains two amino acid substitutions compared with *Af*ChiB1: Thr^{138} is replaced by an asparagine and Tyr^{139} is replaced by a phenylalanine. Despite the relatively conservative nature of these substitutions C_2-dicaffeine inhibits HCHT with an IC_{50} of 107 ± 5 μM, which is 1.3 orders of magnitude weaker compared with its inhibition of *Af*ChiB1. Thr^{138} and Tyr^{139} form one wall of the subsite binding the secondary caffeine, and whereas their side chains do not form hydrogen bonds with the ligand, they make extensive van der Waals interactions that are likely to contribute significantly to ligand binding and stabilization. Crystal structures of HCHT (17, 34) show that the asparagine replacing Thr^{138} adopts a conformation similar to that of the threonine and thus is unlikely to significantly alter binding. On the other hand, the side chain of the phenylalanine replacing Tyr^{139} points away from the active site, into a pocket created by a glycine in place of *Af*ChiB1 Asn^{78}. This leaves the binding site for the secondary caffeine more open, explaining the reduced affinity of HCHT for C_2-dicaffeine, especially considering that "monocaffeine" ligands like theophylline or pentoxifylline bind more tightly to HCHT compared with *Af*ChiB1.

Mouse (and human) acidic mammalian chitinase carry the same two substitutions as HCHT; additionally Arg^{301} is replaced by a histidine and a glutamine takes the place of Glu^{322}. The IC_{50} for C_2-dicaffeine against mouse lung acidic mammalian chitinase activity is 90 ± 4 μM, which is similar to the value obtained for HCHT, suggesting that neither the arginine to histidine substitution nor the replacement of Glu^{322}, which does not directly interact with the dicaffeine ligand, significantly influence ligand binding.

*Sm*ChiA differs from *Af*ChiB1 in only one active site residue, Tyr^{139} is replaced by a leucine. Still, this substitution increases the IC_{50} for C_2-dicaffeine against *Sm*ChiA to 71 ± 3 μM. Inspection of *Sm*ChiA crystal structures (*e.g.* PDB code 1CTN (35)) shows that the smaller leucine side chain could not reach a C_2-dicaffeine ligand bound in the conformation observed for *Af*ChiB. This again results in a loss of van der Waals interactions, thus explaining the reduced affinity of the dicaffeine for *Sm*ChiA compared with *Af*ChiB1.

Whereas the wide conservation of the three "essential" tryptophans among bacterial-like family 18 chitinases suggests that the dicaffeine molecule provides a useful general scaffold for the generation of inhibitors against this group of enzymes, comparisons of several family 18 members reveal that relatively subtle changes in active site construction can significantly affect affinity. This makes it likely that dicaffeine derivatives selective for only a small number or even individual family 18 targets can be designed. It should also be noted that the conservation of active site features among bacterial-like family 18 chitinases does not extend to their "plant-like" siblings: most *Af*ChiB1 active site residues, including the three tryptophans, are conserved in less than 15% of plant-like family 18 chitinase sequences.

DISCUSSION

This work presents an approach to performing rapid virtual screening experiments based on the known conformation of a ligand fragment in a target binding site, as well as the application of this method to elaborate a methylxanthine fragment common to several recently identified inhibitors of *Af*ChiB1 (19). Whereas the method identifies both known and novel *Af*ChiB1 inhibitors, a large number of predicted hits turn out to be false positives, which is unexpected, in particular as the assumptions made to speed up the virtual screening should, if anything, give rise to false negative results. To re-evaluate the results, the compounds in Table 1 were re-docked using AutoDock 3.0, which uses essentially the same force field as LIGTOR, but, while slower than LIGTOR, is better suited to *ab initio* docking and produces a list

of favorable conformations instead of a single "best" conformation. Table 1 identifies the AutoDock cluster (re-ranked by ΔG) most similar to the LIGTOR-generated pose and the r.m.s. deviation between the two conformations. The results suggest that the large number of false positives is not due to a shortcoming of the employed docking protocol, but instead most likely stems from problems of the force field employed. At the same time the data indicate that the assumption that the fragment substructure binds to the active site in a fixed conformation may not hold in all cases, in particular for compounds with large extensions like **3**, **4**, or **6**. In addition, the rapid evaluation with LIGTOR may not find the desired energy minimum in cases of highly flexible attachments, as seen in the case of compound **6**, leading to an expected increase of false negatives. To improve the predictions from the virtual screen, the use of a separate scoring function is being investigated. Alternatively, a small number of candidate ligands could be evaluated using free-energy perturbation calculations (36).

LIGTOR together with PRODRG provides a simple affinity grid-based docking implementation. It can be used as a building block for a variety of docking protocols, including the fragment-based approach described here, but also for evaluating a series of synthesizable compounds, in ligand growing protocols or for fitting ligands to electron density maps.[5] It should also be noted that the grid-based docking as implemented by LIGTOR is relatively force field agnostic and more elaborate force fields could be adopted with little effort.

The newly identified dicaffeine compound represents a promising starting point for the design of family 18 chitinase inhibitors. With a molecular mass of 386 Da, a cLogP of −0.77, six hydrogen bond acceptors, and no hydrogen bond donors, it conforms with Lipinski's rule of five (37). It also is reasonably rigid, possessing only three free torsions involving non-hydrogen atoms. C_2-dicaffeine can be derivatized in numerous locations, both on the xanthine ring systems and on the linker, and many derivatives are easily synthetically accessible. Sequence comparisons and assays of additional enzymes suggest that the dicaffeine scaffold can form a basis for the design of specific inhibitors of bacterial-like, but not plant-like, family 18 chitinases.

CONCLUSIONS

Family 18 chitinases comprise drug targets from fungal and protozoan pathogens, and also have been implicated as effectors in allergic asthma. Using a new docking program, LIGTOR, a purine fragment common to several previously characterized chitinase inhibitors is elaborated into a new inhibitor, C_2-dicaffeine, which has low micromolar affinity for a model chitinase and desirable drug-like properties. The crystal structure of a C_2-dicaffeine-chitinase complex shows the inhibitor interacting with two separate subsites in the active site cleft and suggests that its scaffold should be widely applicable to the development of specific inhibitors of family 18 chitinases.

[5] A. W. Schüttelkopf, unpublished data.

Acknowledgment—We thank the European Synchrotron Radiation Facility, Grenoble, for the time on beamline BM14.

REFERENCES

1. Thompson, J. D., Higgins, D. G., and Gibson, T. J. (1994) *Nucleic Acids Res.* **22,** 4673–4680
2. Cabib, E., Silverman, S. J., and Shaw, J. A. (1992) *J. Gen. Microbiol.* **138,** 97–102
3. Kuranda, M. J., and Robbins, P. W. (1991) *J. Biol. Chem.* **266,** 19758–19767
4. Takaya, N., Yamazaki, D., Horiuchi, H., Ohta, A., and Takagi, M. (1998) *Biosci. Biotechnol. Biochem.* **62,** 60–65
5. Hollak, C. E. M., van Weely, S., van Oers, M. H. J., and Aerts, J. M. F. G. (1994) *J. Clin. Investig.* **93,** 1288–1292
6. Boot, R. G., Renkema, G. H., Verhoek, M., Strijland, A., Bliek, J., de Meulemeester, T. M. A. M. O., Mannens, M. M. A. M., and Aerts, J. M. F. G. (1998) *J. Biol. Chem.* **273,** 25680–25685
7. Labadaridis, I., Dimitriou, E., Theodorakis, M., Kafalidis, G., Velegraki, A., and Michelakakis, H. (2005) *Arch. Dis. Child.* **90,** F531–F532
8. Guo, Y., He, W., Boer, A. M., Wevers, R. A., de Bruijn, A. M., Groener, J. E., Hollak, C. E., Aerts, J. M., Galjaard, H., and van Diggelen, O. P. (1995) *J. Inherit. Metab. Dis.* **18,** 717–722
9. Andersen, O. A., Dixon, M. J., Eggleston, I. M., and van Aalten, D. M. F. (2005) *Nat. Prod. Rep.* **22,** 563–579
10. Izumida, H., Imamura, N., and Sano, H. (1996) *J. Antibiot.* **49,** 76–80
11. Houston, D. R., Eggleston, I., Synstad, B., Eijsink, V. G. H., and van Aalten, D. M. F. (2002) *Biochem. J.* **368,** 23–27
12. Arai, N., Shiomi, K., Yamaguchi, Y., Masuma, R., Iwai, Y., Turberg, A., Koelbl, H., and Omura, S. (2000) *Chem. Pharm. Bull.* **48,** 1442–1446
13. Shiomi, K., Arai, N., Iwai, Y., Turberg, A., Koelbl, H., and Omura, S. (2000) *Tetrahedron Lett.* **41,** 2141–2143
14. Houston, D. R., Shiomi, K., Arai, N., Omura, S., Peter, M. G., Turberg, A., Synstad, B., Eijsink, V. G. H., and van Aalten, D. M. F. (2002) *Proc. Natl. Acad. Sci. U. S. A.* **99,** 9127–9132
15. Sakuda, S., Isogai, A., Matsumoto, S., Suzuki, A., and Koseki, K. (1986) *Tetrahedron Lett.* **27,** 2475–2478
16. Terwisscha van Scheltinga, A. C., Armand, S., Kalk, K. H., Isogai, A., Henrissat, B., and Dijkstra, B. W. (1995) *Biochemistry* **34,** 15619–15623
17. Rao, F. V., Houston, D. R., Boot, R. G., Aerts, J. M. F. G., Sakuda, S., and van Aalten, D. M. F. (2003) *J. Biol. Chem.* **278,** 20110–20116
18. Rao, F. V., Houston, D. R., Boot, R. G., Aerts, J. M. F. G., Hodkinson, M., Adams, D. J., Shiomi, K., Omura, S., and van Aalten, D. M. F. (2005) *Chem. Biol.* **12,** 65–76
19. Rao, F. V., Andersen, O. A., Vora, K. A., DeMartino, J. A., and van Aalten, D. M. F. (2005) *Chem. Biol.* **12,** 973–980
20. Erlanson, D. A., McDowell, R. S., and O'Brien, T. (2004) *J. Med. Chem.* **47,** 3463–3482
21. Carr, R. A. E., Congreve, M., Murray, C. W., and Rees, D. C. (2005) *Drug Discov. Today* **10,** 987–992
22. Schüttelkopf, A. W., and van Aalten, D. M. F. (2004) *Acta Crystallogr. Sect. D Biol. Crystallogr.* **60,** 1355–1363
23. Morris, G. M., Goodsell, D. S., Halliday, R., Huey, R., Hart, W. E., Belew, R. K., and Olson, A. J. (1998) *J. Comp. Chem.* **19,** 1639–1662
24. Cavallaro, R. A., Filocamo, L., Galuppi, A., Galioni, A., Brufani, M., and Genazzani, A. A. (1999) *J. Med. Chem.* **42,** 2527–2534
25. Leatherbarrow, R. J. (2001) *GraFit*, Version 5, Erithacus Software Ltd., Horley, UK
26. Otwinowski, Z., and Minor, W. (1997) *Methods Enzymol.* **276,** 307–326
27. Jones, T. A., Zou, J. Y., Cowan, S. W., and Kjeldgaard, M. (1991) *Acta Crystallogr. Sect. A* **47,** 110–119
28. Murshudov, G. N., Vagin, A. A., and Dodson, E. J. (1997) *Acta Crystallogr. Sect. D Biol. Crystallogr.* **53,** 240–255
29. Hopkins, A. L., Groom, C. R., and Alex, A. (2004) *Drug Discov. Today* **9,** 430–431

30. Gray, N., Detivaud, L., Doerig, C., and Meijer, L. (1999) *Curr. Med. Chem.* **6,** 859–875
31. Chiosis, G., Lucas, B., Huezo, H., Solit, D., Basso, A., and Rosen, N. (2003) *Curr. Cancer Drug Targets* **3,** 371–376
32. Braendvang, M., and Gundersen, L. L. (2005) *Bioorg. Med. Chem.* **13,** 6360–6373
33. Vivet-Boudou, V., Didierjean, J., Isel, C., and Marquet, R. (2006) *Cell. Mol. Life Sci.* **63,** 163–186
34. Fusetti, F., von Moeller, H., Houston, D., Rozeboom, H. J., Dijkstra, B. W., Boot, R. G., Aerts, J. M. F., and van Aalten, D. M. F. (2002) *J. Biol. Chem.* **277,** 25537–25544
35. Perrakis, A., Tews, I., Dauter, Z., Oppenheim, A. B., Chet, I., Wilson, K. S., and Vorgias, C. E. (1994) *Structure* **2,** 1169–1180
36. Kollman, P. (1993) *Chem. Rev.* **93,** 2395–2417
37. Lipinski, C. A., Lombardo, F., Dominy, B. W., and Feeney, P. J. (1997) *Adv. Drug Delivery Rev.* **23,** 3–25